REPRODUCTION
RESEARCH

Normotensive rats with PCOS exhibit the hypertensive pattern: focus on oxidative stress

Jovana Joksimovic Jovic[1], Nikola Jovic[2], Jasmina Sretenovic[1], Vladimir Zivkovic[1], Maja Nikolic[1], Jovan Rudic[3], Verica Milošević[4], Nataša Ristić[4], Kristina Andric[5], Tijana Dimkic Tomic[6], Biljana Milicic[7] and Vladimir Jakovljevic[1,8]

[1]Department of Physiology, Faculty of Medical Sciences, University of Kragujevac, Kragujevac, Serbia, [2]Department of Gynecology and Obstetrics, Faculty of Medical Sciences, University of Kragujevac, Kragujevac, Serbia, [3]University Clinic for Gynecology and Obstetrics 'Narodni Front', Belgrade, Serbia, [4]Department of Cytology, Institute for Biological Research 'Siniša Stanković' – National Institute of Republic of Serbia, University of Belgrade, Belgrade, Serbia, [5]Department of Dermatovenerology, Faculty of Medical Sciences, University of Kragujevac, Kragujevac, Serbia, [6]Clinic for Rehabilitation 'Dr Miroslav Zotović', Belgrade, Serbia, [7]Department for Medical Statistics and Informatics, School of Dental Medicine, University of Belgrade, Belgrade, Serbia and [8]Department of Human Pathology, I.M. Sechenoov First Moscow State Medical University, Moscow, Russia

Correspondence should be addressed to J Joksimovic Jovic; Email: jovana_joksimovic@yahoo.com

Abstract

Numerous evidence implies complex interrelations between polycystic ovary syndrome (PCOS) and hypertension (HT) in reproductive-age women. In this study, we aimed to investigate the potential strain differences in ovarian morphology, hemodynamic, and biochemical characteristics in an androgen-induced PCOS rat model. A total of 24 rats of 3 weeks old (12 Wistar Kyoto – WK and 12 spontaneously hypertensive rats – SHR) were divided into four groups: WK, WK PCOS, SHR, and SHR PCOS. PCOS was induced by daily s.c. injections of testosterone enanthate (1 mg/100 g body weight) administered for 5 weeks. PCOS induction led to estrus cyclicity cessation, cystic ovarian appearance, and sex hormones disturbances in both strains. The morphometric parameters in ovaries were altered in a manner of PCOS-related changes in both strains (higher number in preantral, atretic, and cystic follicles). Ultrasonographically, a significant decrease in ovarian volume (OV) was registered in PCOS groups but also in SHR compared to WK rats. All blood pressure parameters were higher in SHR compared to WK. PCOS modeling increased systolic, mean arterial, and pulse pressure in WK strain, while in SHR, only mean arterial and pulse pressure were higher. Alterations in oxidative stress parameters could provide a molecular basis for PCOS-related changes: in PCOS groups, thiobarbituric acid reactive substance and superoxide anion radical levels were higher in both strains, while superoxide dismutase and glutathione were significantly lowered.

Reproduction (2022) **163** 11–21

Introduction

Although polycystic ovaries were first recognized in the early 1900, the polycystic ovary syndrome (PCOS), as the most common endocrinopathy among reproductive-age women, represents the phenomenon of the 20th century (Rodgers *et al.* 2019). The presence of two of three Rotterdam criteria: hyperandrogenism (clinical and/or biochemical), oligo-, and/or ameno-rrhea, and ultrasonographically verified ovarian cysts has been used since 2004 for PCOS diagnosing.

Unfortunately, PCOS patients frequently remain undiagnosed, therefore they usually face severe complications, such as hypertension (HT); PCOS women frequently experience higher blood pressure (BP) levels (Elting *et al.* 2001, Orio *et al.* 2006, Wang *et al.* 2012). Although obesity could be considered the joint feature for these two disorders, the fact that lean or non-obese PCOS women might also develop HT (Marchesan & Spritzer 2019, Zhu *et al.* 2019) further excludes obesity as the main constituent, putting in focus other potential mechanisms involved. The higher activity of the sympathetic nervous system is considered to have a significant role in HT pathogenesis, which was also recognized in PCOS (Lansdown & Rees 2012). Besides, the lower birth weight has been associated with a higher risk for both PCOS and HN development in adulthood (IJzerman *et al.* 2003, Mumm *et al.* 2013). Even though the high level of androgens is associated with higher BP (Chen *et al.* 2007), whether HT influences PCOS development remains elusive. Oxidative stress (OS) was recognized as one of the most common underlying pathophysiological mechanisms in PCOS (Zuo *et al.* 2016). Furthermore, OS could be related to

ISSN 1470–1626 (paper) 1741–7899 (online)
https://doi.org/10.1530/REP-21-0219
Online version via https://rep.bioscientifica.com

HT development, impairing redox-dependent vascular signaling (Münzel *et al.* 2017).

PCOS animal models usually exhibit a combination of two or more PCOS-like equivalents of Rotterdam criteria that qualify them as useful and provide potential relevance for etiopathogenic studies (Stener-Victorin *et al.* 2020). However, literature data arguably indicate that none of them fully encompass all the clinical symptoms in PCOS women. Although different types of androgens were commonly used for PCOS modeling in rats, postnatal testosterone-induced PCOS models seem to be more appropriate than prenatal, showing typical human PCOS features of acyclicity, anovulation, polycystic ovaries, hyperandrogenism, and insulin resistance (Walters *et al.* 2012, Joksimovic Jovic *et al.* 2021). Spontaneously hypertensive rats (SHR) represent the strain with the congenital tendency for HT development from the age of 4 weeks and established HT in adult age. Moreover, SHR already poses reproductive abnormalities, such as delayed puberty and various hormonal disturbances (Pinilla *et al.* 1992, 2009), and increased sympathetic activity (Martínes *et al.* 2019), which makes them an inevitable strain in studies concerning reproduction and HT.

Considering the abovementioned facts, the aim of this study was to investigate the differences in ovarian characteristics, BP, hormonal status, and OS parameters in normotensive rats and SHR in the PCOS model.

Materials and methods

Animals

Weaning Wistar Kyoto (WK) and SHR dams were purchased with 14-day-old pups from the Military Medical Academy, Belgrade, Serbia. After 7 days of acclimatization, 21-day-old normotensive WK rats ($n = 12$) and SHR ($n = 12$), weighing 50–60 g, were enrolled in the experimental protocol. Rats were kept under controlled environmental conditions (23 ± 1°C, 12 h light:12 h darkness cycle – lights on 8:00 h), with access to food and water *ad libitum*. All research procedures were carried out in strict accordance with the European Directive for the welfare of laboratory animals No. 86/609/EEC and principles of Good Laboratory Practice and ARRIVE guidelines. Ethical approval was obtained from the Ethical Committee of the Faculty of Medical Sciences, University of Kragujevac, Serbia. Efforts were made to minimize the number of animals used and their suffering.

Experimental design

WK rats, as well as SHR, were randomly divided into two groups (six animals per group): WK control group (WK), WK PCOS group (WK PCOS), SHR control group (SHR), and SHR PCOS group (SHR PCOS). PCOS was induced by daily s.c. injection of testosterone enanthate (TE, Galenika a.d., Serbia), dissolved in sesame oil (1 mg/100 g body weight (BW)), starting from the age of 21 days (prepubertal) to 5 weeks (Ghowsi *et al.* 2018). Animals from control groups received 0.1 mL sesame oil for 5 weeks. After cessation of protocol, animals were anesthetized by i.p. application of ketamine (10 mg/kg) and xylazine (5 mg/kg) and sacrificed by decapitation on the guillotine for further trunk blood and ovarian tissue collection. The left ovary was excised from connective and fat tissue, washed in cold saline, weighed, photographed, and prepared for further histological analysis.

Trunk blood was collected in two separate tubes. Serum was obtained after allowing blood to clot in anticoagulant-free tubes at room temperature for 2 h and then centrifuged at 3500 ***g*** for 15 min at 4°C. The clear supernatant was kept at −80°C until analysis. Plasma was obtained after centrifugation of blood in tubes with sodium citrate. All animals were sacrificed at the same estrus cycle phase (diestrus) to eliminate the impact of the hormonal alterations on analyzed parameters.

Assessment of estrus cycle

During the last 8 days of protocol, the estrus cycle was monitored daily by cytological examination of vaginal smears. Briefly, every morning at 9:00 h, before treatment, vaginal lavage was performed by dropper filled with a small volume of distilled water. The lavage was placed on a glass slide, stained with hematoxylin, and analyzed by a light microscope. Estrus cycle phases were identified by predomination of specific cells: proestrus – round, nucleated cells; estrus – cornified squamous cells; metaestrus – cornified squamous cells and leucocytes; and diestrus – nucleated epithelial cell and predominance of leucocytes (Marcondes *et al.* 2002).

Hormonal assays

Commercial ELISA kits (Elecsys testosterone II, estradiol III, and progesterone II, Roche Diagnostics) were used to determine serum levels of testosterone (T), estradiol (E2), and progesterone (P4). T, E2, and P4 levels were determined using the Elecsys 2010 analyzer by the electrochemiluminescence immunoassay method. T and P4 levels were expressed in ng/mL, and E2 was expressed in pg/mL. The sensitivities of the assays for T, P4, and E2 were 0.025, 0.03, and 5 pg/mL, respectively. Inter- and intra-assay coefficients of variance for T, P4, and E2 were 3.8, 3, and 2.2%, and 5, 5, and 3.9%, respectively.

Evaluation of arterial blood pressure levels

A day before sacrificing, a non-invasive method for the determination of systolic and diastolic arterial BP and heart rate in rats was performed using BP system (Rat Tail Cuff Method Blood pressure Systems (MRBP-R), IITC Life Science Inc., Los Angeles, CA, USA) (Feng *et al.* 2008). Mean blood pressure (MAP) was determined by the formula: MAP = (systolic BP + (2 × diastolic BP))/3. Pulse pressure (PP) was calculated as the difference between systolic and diastolic BP.

Ultrasound examination of ovaries

At the end of the experimental protocol, the left ovary was ultrasound-examined using Hewlett Packard Sonos 5500 (Andover, MA, USA). Before examination, rats were

anaesthetized using ketamine (50 mg/kg) and xylazine (10 mg/kg). The sector scanner equipped with a 15.0 MHz phased array linear transducer (1.5 cm aperture) was used for visualization of the ovaries. Transabdominal view in two-dimensional mode, and B-mode, localized ovaries topographically beside kidneys and toward echogenic characteristics. Three ovary dimensions were measured, and ovary volume (mm^3) was calculated by the prolate ellipsoid formula where the volume is the product of $\pi/6$ and the longitudinal (D1), transversal (D2), and anteroposterior (D3) diameters (volume $= \pi/6$ (D1 × D2 × D3)) (Nardo *et al.* 2003). The left ovary was measured and analyzed to correlate ultrasonographically the obtained results with the following histological examination.

Oxidative stress markers

Index of lipid peroxidation

The degree of lipid peroxidation in the plasma samples was estimated by measuring thiobarbituric acid reactive substances (TBARS) using 1% thiobarbituric acid in 0.05 NaOH, incubated with the plasma samples at 100°C for 15 min, and measured at 530 nm. Distilled water solution with 1% thiobarbituric acid in 0.05 NaOH served as a blank probe (Ohkawa *et al.* 1979).

Determination of nitrites

The method for detection of the plasma nitrate and nitrites (NO_2^-) levels is based on the Griess reaction. NO_2^- was determined as an index of NO production with Griess reagent (Green *et al.* 1982). 0.1 mL of 3 N perchloride acid, 0.4 mL of 20 mmol/L ethylenediaminetetraacetic acid (EDTA), and 0.2 mL of plasma were put on ice for 15 min and then centrifuged for 15 min at 4000 ***g*** After discarding the supernatant, 220 µL K_2CO_3 was added. NO_2^- was measured at 550 nm. Distilled water was used as a blank probe.

Determination of hydrogen peroxide

The measurement of hydrogen peroxide (H_2O_2) is based on the oxidation of phenol red by hydrogen peroxide in a reaction catalyzed by horseradish peroxidase (HRPO). Plasma sample of 200 µL was precipitated with 800 µL of freshly prepared phenol red solution, followed by the addition of 10 µL of (1:20) HRPO (made ex tempore). Distilled water was used as blank probe instead of plasma samples. The level of H_2O_2 was measured at 610 nm (Pick & Keisari 1980)

Determination of superoxide anion radical

The superoxide anion radical (O_2^-) concentration was measured after the reaction of nitro blue tetrazolium in tris (hydroxymethyl) aminomethane buffer with the plasma samples, at 530 nm. Distilled water solution was used as a blank probe (Auclair & Voisin 1985).

Determination of antioxidant enzymes

Isolated red blood cells were washed three times with three volumes of ice-cold 0.9 mmol/L NaCl. Hemolysates containing about 50 g Hb/L were prepared (McCord & Fridovich 1969) and used to determine catalase (CAT) activity. CAT activity was determined according to Beutler (1982). Detection was performed at 360 nm. Distilled water was used as a blank probe. Superoxide dismutase (SOD) activity was determined by the epinephrine method (Misra & Fridovich 1972). Lysate of 100 µL and 1 mL carbonate buffer were mixed, and then, 100 µL of epinephrine was added. Detection was performed at 470 nm.

Determination of reduced glutathione

Glutathione (GSH) was determined spectrophotometrically, and it is based on GSH oxidation via 5.5-dithiobis-6.2-nitrobenzoic acid. GSH extract was obtained by combining 0.1 mL of 0.1% EDTA, 400 µL of plasma, and 750 µL of precipitation solution (containing 1.67 g metaphosphoric acid, 0.2 g EDTA, 30 g NaCl, and filled with distilled water to 100 mL; the solution is stable for 3 weeks at 4°C). After mixing in the vortex machine and extracting on cold ice (15 min), it was centrifuged at 1800 ***g*** (10 min). Distilled water was used as a blank probe. Measuring was performed at 420 nm (Beutler 1984).

Tissue processing and histomorphometry

The left ovaries were fixed overnight in the 10% neutral formalin and dehydrated in increasing concentrations of ethanol, immersed in xylene, and finally embedded in paraffin. Tissue blocks were serially sectioned at 3 µm of thickness, stained with hematoxylin and eosin, and subjected to light microscopic analysis. Three sections per ovary, corresponding approximately to 150 µm in front and behind the central section, were selected for follicle quantification (Qiu *et al.* 2009). Only follicles with visible oocyte and nucleus were counted. The follicles were classified as follows: preantral, (healthy) antral, and atretic follicles, according to (Liu *et al.* 2005). The number of corpus luteum (CL) and the number of cystic follicles (CF) were counted from the largest section. The criteria for cystic follicle identification were: one to four layers of granulosa cells (GC), with no luteinization, thin wall consisting of thin flattened cell resting on thin fibrous capsule, larger than normal preovulatory follicle, and degeneration of individual GC (Simão *et al.* 2016). In addition, the following parameters were obtained from the largest section, using calibrated Axiovision software (Zeiss) for morphometric analysis: longitudinal ovarian diameter and thickness of GC and theca cells (TC) layers of the largest follicle from three different visual fields. Two persons performed the follicle counting independently, at Olympus BX 51 microscope, using 100× and 400× magnification. First, the results per single rat ovary were pooled, and then, results from six animals were pooled to obtain group means.

Statistical analysis

Values were presented as the means (S.D.) and 95% CI. A normal distribution of all numeric data was tested using the Koglomorov–Smirnov test. If the data were normally distributed, two-way ANOVA was used. Non-parametric data were analyzed using the Kruskal–Wallis followed by *post hoc* Mann–Whitney test. Analysis of BW was performed using the Fridman test for comparing BWs within a group at different time

points, followed by *post hoc* Wilcoxon test. Kruskal–Wallis with *post hoc* analysis was performed to analyze intergroup differences of BW, at different time-point measurements. All analyses were carried out using SPSS statistical program version 27.0. The *P* value below 0.05 is considered statistically significant.

Results

Body weight

During the 5-week protocol, BW differed significantly in all groups (Fig. 1A). All four groups had a significant weekly time-point increase of BW during 5 weeks of protocol ($P < 0.01$, not presented in Fig. 1A). The evaluation of the BW between groups showed that WK and WK PCOS groups differed significantly ($P < 0.05$) in the 4th (33%) and 5th (21%) week. However, strain differences were observed regarding WK and SHR groups in all time-point measurements ($P < 0.01$) and regarding WK PCOS and SHR PCOS group ($P < 0.01$, Fig. 1A). Moreover, the differences between SHR and SHR PCOS groups were not registered during the protocol.

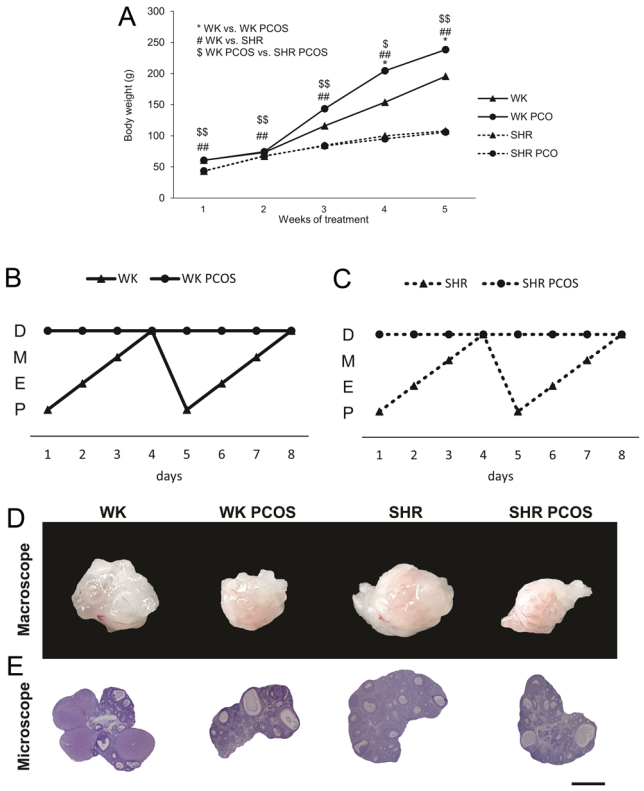

Figure 1 PCOS characteristics of rats from WK, WK PCOS, SHR, and SHR PCOS groups. (A) Body weight (BW) alterations during 5-week treatment period; (B) estrus cycle in WK strain, with or without PCOS induction; P, pro-estrus; E, estrus; M, metestrus; D, diestrus; (C) estrus cycle in SHR strain, with or without PCOS induction; P, pro-estrus; E, estrus; M, metestrus; D, diestrus; (D) macroscopic ovarian appearances; (E) microphotographs of the largest ovarian section (magnification 5×, scale bar = 400μm). Intergroup comparations were performed using Kruskal–Wallis test and *post hoc* Mann–Whitney analysis: $^{*}P < 0.05$ – WK vs WK PCOS, $^{\#}P < 0.05$ ($^{\#\#}P < 0.01$) – WK vs SHR, $^{\$}P < 0.05$ ($^{\$\$}P < 0.01$) – WK PCOS vs SHR PCOS. Repeated measure ANOVA was used for statistical analysis of BW within the groups; all groups showed statistically significant increase through time (significances were not presented in the graph).

Estrus cycle

Both WK and SHR expressed regular cycles of 4–5 days duration (100% of rats from both groups cycled). However, PCOS induction led to the cessation of estrus cycle in both WK PCOS and SHR PCOS groups (Fig. 1B and C).

Macroscopic ovarian appearance is represented in Fig. 1D. There was an evident decrease in ovarian size in the WK PCOS group compared to WK and in the SHR PCOS group compared to SHR. Cystic ovarian appearance was evident in both PCOS groups.

Microphotographs of the largest ovarian sections are presented in Fig. 1E. Normal morphology of ovaries was shown in the WK group: follicles in different follicular development stage, presence of corpora lutea (CL), and absence of cystic follicles (CF). On the other hand, the WK PCOS rats showed the presence of cystic and numerous atretic follicles, absence of CL, and a marked decrease in the area of the largest section. SHR strain was characterized by numerous atretic follicles compared to the WK strain, but with the presence of few CL in SHR, unlike in SHR PCOS group which was without any CL.

The ultrasound evaluation of left ovary

The ultrasonographical examination of ovaries showed no differences in D1, D2, and D3 regarding strain differences. However, after PCOS induction, there was a decrease in D1 (29% in WK and 22% in SHR, $P < 0.01$) and D3 (14% in WK and 9% in SHR strain $P < 0.01$) (Fig. 2A and C), while D2 did not differ significantly (Fig. 2B). Ovary volume (OV) analysis showed significantly lower values in SHR compared to the WK group (15%, $P < 0.01$). In addition, OV was lowered significantly ($P < 0.01$) between PCOS and matched-control groups in WK and SHR strains (43 and 29%, respectively), as shown in Fig. 2D, without difference regarding strain. However, the OV/BW index showed differences between observed groups regarding both strain and PCOS induction, although without significant interaction strain×PCOS ($P > 0.05$) (Fig. 2E). Representative ultrasonographical images of left rat ovaries from all investigated groups are presented in Fig. 2F. In all investigated groups, ovaries are shown as oval, clearly demarcated isoechoic formations. It was observed that D1 of both control groups was higher compared to the PCOS groups. In both PCOS groups, hypoechoic circular formations could be observed, which could correspond to cysts (fluid-filled cavities) according to ultrasound characteristics. The

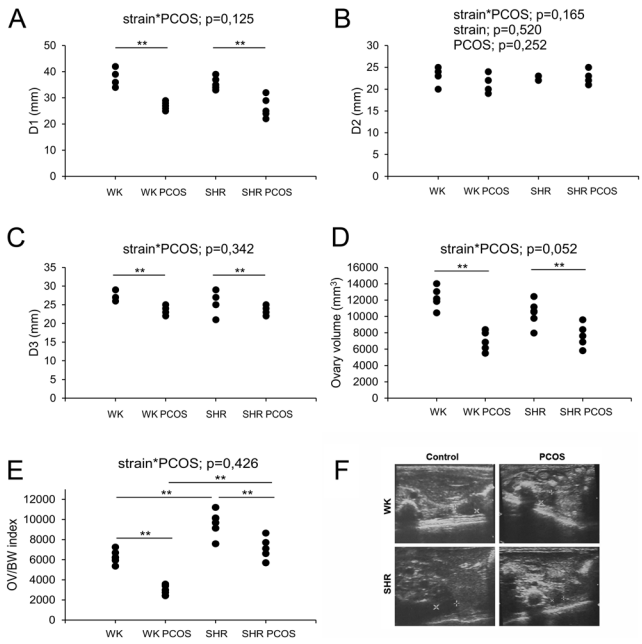

Figure 2 Ultrasonographic evaluation of ovarian measurements in rats from WK, WK PCOS, SHR, and SHR PCOS groups. (A) Longinudinal ovarian diameter – D1; (B) transversal ovarian diameter – D2; (C) anteroposterior ovarian diameter – D3; (D) ovary volume; (E) ovary volume/body weight (OV/BW) index; (F) representative ultrasonographical images of left rat ovaries from all investigated groups. $^{**}P < 0.05$, two-way ANOVA was used for analysis; factor strain and factor PCOS were evaluated.

ovarian stroma of both PCOS groups has hyperechoic fields, especially in WK PCOS, that would correspond to the foci of atretic follicles and hypertecosis.

Number of follicles and morphometric analysis in rat ovary

The number of preantral, atretic, and cystic follicles was significantly higher ($P < 0.01$) in SHR compared to WK rats (Table 1). Also, PCOS groups depicted higher ($P < 0.01$) values of these parameters in both strains. On the other hand, the number of healthy antral follicles was lowered ($P < 0.01$) in SHR compared to WK, as well as in PCOS groups ($P < 0.01$) compared to respective controls.

Diameters of central ovarian sections were analyzed and a significant decrease after PCOS induction was observed in both strains ($P < 0.01$), while there was no change regarding strain differences (Table 1). The thickness of the granulosa layer was similar in WK and SHR, but theca was thickened in SHR compared to WK ($P < 0.01$). PCOS induction decreased granulosa layer thickness in both strains ($P < 0.01$), while theca was increased ($P < 0.01$) only in the WK. The number of CL and tertiary follicles (TF) was significantly lower in SHR compared to WK ($P < 0.01$), and PCOS modeling led to a decrease in CL and TF in both strains.

Serum hormone levels

PCOS induction in both strains induced significant ($P < 0.01$) elevation in serum T levels, compared to respective control rats. Also, serum T level was significantly ($P < 0.01$) higher in SHR compared to WK group (Fig. 3A). P4 was significantly ($P < 0.01$) lower in SHR compared to WK (Fig. 3B), while PCOS induction significantly ($P < 0.01$) reduced P4 levels in WK and SHR strain. E2 levels were significantly ($P < 0.01$) higher in both strains after PCOS induction compared to respective control groups (Fig. 3C).

Blood pressure and heart rate

As shown in Fig. 4A and B, both systolic and diastolic arterial BPs were significantly ($P < 0.01$) higher (26 and 14%, respectively) in SHR compared to WK. In contrast, PCOS induction significantly ($P < 0.01$) elevated systolic BP only in WK strain (22%). Heart rate was higher ($P < 0.01$) in both strains after PCOS induction (14% in WK and 6% in SHR strain; Fig. 4C). MAP was significantly higher ($P < 0.01$) regarding strain differences (19% SHR vs WK and 7% SHR PCOS vs WK PCOS) and PCOS induction (14% in WK strain and 3% in SHR strain), as shown in Fig. 4D. A significant interaction between two factors was registered regarding MAP (strain×PCOS; $P < 0.01$). PP was significantly higher ($P < 0.01$) regarding strain differences (54% SHR vs WK and 19% SHR PCOS vs WK PCOS) and PCOS induction (55% in WK strain and 19% in SHR strain), as shown in Fig. 4E.

Oxidative stress markers

PCOS induction led to an increase of TBARS in plasma of WK (45%, $P < 0.01$) and SHR (154, $P < 0.01$). Moreover, TBARS was higher ($P < 0.01$) in SHR compared to WK rats (50%) and in SHR PCOS compared to WK PCOS (162%) (Fig. 5A). Increase ($P < 0.01$) in plasma O_2^- levels was observed regarding strain and PCOS induction (Fig. 5B): SHR showed an increase by 45% when compared to WK and by 34% when SHR PCOS was compared to WK PCOS. The increase was observed in PCOS groups of WK and SHR strain compared to their respective controls (39 and 28%, respectively). Levels of nitrites were higher ($P < 0.01$) by strain (16% in SHR and 53% in SHR PCOS), and significant interaction between analyzed factors was registered (strain×PCOS; $P < 0.01$), as shown in Fig. 5C. H_2O_2 levels were higher by strain ($P < 0.01$) in SHR (97%) and in SHR PCOS (162%), while PCOS modeling did not alter H_2O_2 levels in both strains compared to respective controls (Fig. 5D).

SOD levels (Fig. 5E) were significantly lowered ($P < 0.01$) by strain in SHR (34%) and in SHR PCOS (38%) and by treatment in WK PCOS (53%) and SHR PCOS (100%) compared to respective controls. As shown

Table 1 Analysis of morphological paramaters in ovaries of rats from WK, WK PCOS, SHR, and SHR PCOS groups. Values are expressed as the means (S.D.) and 95% CI. Two-way ANOVA was used for the analysis of thickness of granulosa layer and diameter of central ovarian section (strainxPCOS; $P = 0.232$ and $P = 0.164$, respectively); Kruskal–Wallis test followed by Mann–Whitney *post hoc* analysis was used for analysis other parameters.

	WK		WK PCOS		SHR		SHR PCOS	
Parameter	Mean (S.D.)	95% CI	Mean (S.D.)	95% CI	Mean (S.D.)	95% CI	Mean (S.D.)	95% CI
Number of preantral follicles	7.28 (1.53)	6.52–8.04	12.06 (2.55)^{a}	10.79–13.3	10.89 (2.14)^{a}	9.83–11.95	15.50 (2.33)^{a,b,c}	14.34–16.66
Number of antral follicles	7.06 (1.55)	6.28–7.83	2.61 (0.92)^{a}	2.16–3.07	3.56 (1.79)^{a}	2.67–4.46	2.28 (0.75)^{a,C}	1.90–2.65
Number of atretic follicles	5.89 (2.27)	4.76–7.02	16.72 (3.66)^{a}	14.90–18.54	14.00 (2.14)^{a,B}	12.93–15.07	20.28 (7.02)^{a,c}	16.79–23.77
Diameter of central ovarian section	3402.70 (464.36)	3171.78–3633.63	2440.31 (646.32)^{a}	2118.90–2761.72	3215.10 (272.67)	3079.50–3350.69	2552.57 (329.68)^{c}	2388.62–2716.52
Thickness of granulosa layer	83.69 (16.63)	75.42–91.95	69.35 (10.61)^{a}	64.08–74.63	89.47 (8.05)	85.46–93.47	67.85 (14.28) ^{c}	60.74–74.95
Thickness of theca layer	18.56 (6.74)	15.21–21.91	31.09 (12.89)^{a}	24.68–37.49	43.38 (14.66) ^{a,b}	36.09–50.67	43.09 (13.37)^{a,b}	35.97–50.21
Number of corpora lutea	2.61 (1.14)	2.04–3.18	0.00 (0.00)^{a}	0.00–0.00	0.78 (1.01)^{a,b}	0.28–1.28	0.00 (0.00)^{a,c}	0.00–0.00
Number of cystic follicles	0.00 (0.00)	0.00–0.00	2.28 (0.46)^{a}	2.05–2.51	3.78 (1.00)^{a,b}	3.28–4.28	2.78 (1.00)^{a,c}	2.28–3.28
Number of tertiary follicles	2.33 (0.69)	1.99–2.67	0.78 (0.43)^{a}	0.57–0.99	0.72 (0.46)^{a}	0.49–0.95	0.00 (0.00)^{a,b,c}	0.00–0.00

$^{a}P < 0.01$ compared to WK group; $^{b}P < 0.01$ compared to WK PCOS group; $^{B}P < 0.05$ compared to WK PCOS group; $^{c}P < 0.01$ compared to SHR group; $^{C}P < 0.05$ compared to SHR.

in Fig. 5F, CAT levels were not significantly different between groups. GSH levels were higher ($P < 0.01$) by strain in SHR (41%) and SHR PCOS (90%). However, PCOS induction significantly reduced ($P < 0.01$) GSH levels in WK and SHR strain (48and 42%, respectively), as shown in Fig. 5G.

Discussion

This study investigated ovarian morphology, BP, hormonal status, and OS parameters after PCOS induction in normotensive rats and SHR. Moreover, the well-known differences in reproductive physiology observed in SHR (Pinilla *et al.* 2009) served as the basis for this investigation and led us to explore more deeply the strain differences (SHR vs WK), particularly after PCOS induction. The established PCOS rat model used in this study affected BW, estrus cycle, ovarian characteristics, hormonal and oxidative status, and BP in both strains. Moreover, we reported specific strain differences, while hormonal and oxidative status in SHR could at least partially explain their reproductive abnormalities.

After 5-week protocol, the final BW was higher in WK PCOS than in WK, which corresponds to the obese PCOS phenotype in women. In contrast to men, high androgen levels in women lead to fat tissue accumulation (Pasquali 2006). Rodent studies also confirmed the increase in BW after androgen treatment in female rats (Johansson *et al.* 2010), which corresponds to our results. Throughout the TE protocol, BW in SHR was lower compared to WK-matched controls. According to our results, SHR have lower BW at birth and in adult age compared to their normotensive controls (Dickhout & Lee 1998). However, PCOS induction did not significantly increase the BW in SHR PCOS compared to SHR, in all time-point measurements. There are no studies investigating similar PCOS protocols in intact SHR females, so we could not compare our results with others. However, T-induced BW gain was absent in ovariectomized female rats (Iwasa *et al.* 2017), which puts in focus the role of estrogen in BW gain. Since estrogen levels increased in SHR PCOS group, we could assume that other mechanisms could be responsible for observed results. It is known that SHR strain possesses disturbed energy homeostasis and reduced orexigenic NPY system in hypothalamus, with an enhanced melanocortin system (Furedi *et al.* 2016). In our recent study, treatment with TE led to enhanced MC4 and diminished NPY immunoreactivity in the hippocampus of Wistar Albino rats and decreased serum NPY (Joksimovic *et al.* 2019). Given that 70% of GnRH neurons are activated by α-MSH via direct activation of MC4 receptors (Roa & Herbison 2012), it is likely that MC4 receptors were directly involved in regulating the hypothalamus–pituitary–ovary axis. Moreover, MC4 receptor mRNA was detected in the

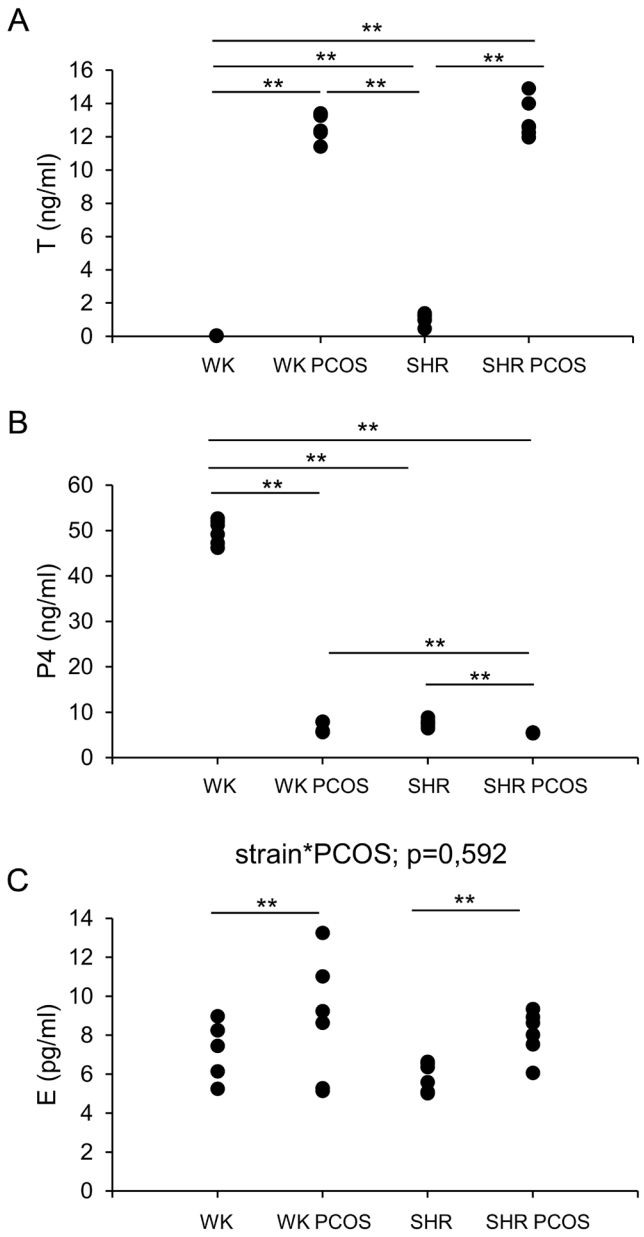

Figure 3 Serum hormone levels in rats from WK, WK PCOS, SHR, and SHR PCOS groups. (A) Levels of testosterone – T; (B) levels of progesterone – P4; (C) levels of estradiol – E2. ** $P < 0.05$, two-way ANOVA was used for the analysis; factor strain and factor PCOS were evaluated or Kruskal–Wallis test and *post hoc* Mann–Whitney analysis were performed.

pituitary and ovaries (Chen *et al.* 2017). On the other hand, it has been shown that SHR females had elevated pituitary (Aguilar *et al.* 1992) and serum FSH levels (Pinilla *et al.* 2009). Similarly, underweight women had higher FSH levels (Aladashvili-Chikvaidze *et al.* 2015). Is the elevated pituitary content of FSH and enhanced melanocortin system in SHR strain responsible for the absence of testosterone-induced BW gain remains to be elucidated in further studies.

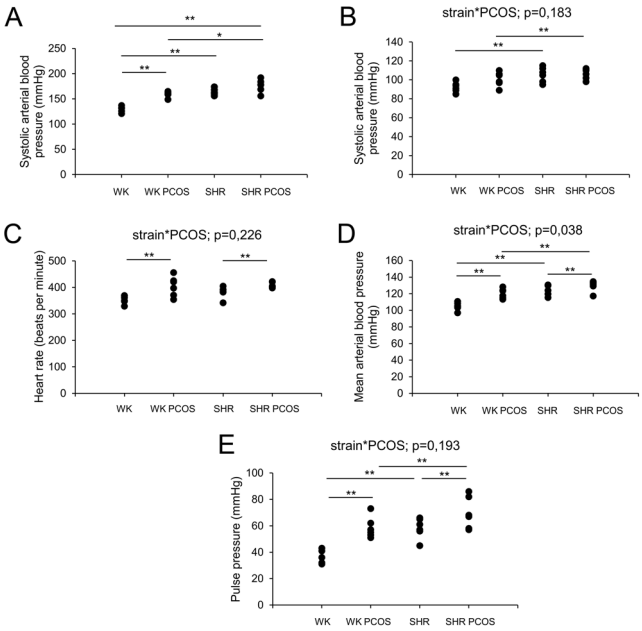

Figure 4 Hemodynamic parameters in rats from WK, WK PCOS, SHR, and SHR PCOS groups. (A) Systolic arterial blood pressure; (B) diastolic arterial blood pressure; (C) heart rate; (D) mean arterial blood pressure; (E) pulse pressure. ** $P < 0.05$, two-way ANOVA was used for analysis; factor strain and factor PCOS were evaluated or Kruskal–Wallis test and *post hoc* Mann–Whitney analysis were performed.

The cessation of estrus cyclicity was registered after PCOS induction in both strains, which corresponds to other studies regarding the PCOS rat model (Ghowsi *et al.* 2018). Even though SHR were found to be different from WK, considering delayed puberty onset and lower ovulation rate, we registered an estrus cycle of normal duration in this strain, which is in accordance with others (Pinilla *et al.* 1992).

Although undetectable T levels in SHR females were reported (Pinilla *et al.* 2009), we registered higher serum T levels in SHR compared to WK. Elevated T levels in the PCOS groups were expected and were in line with other studies (Kalhori *et al.* 2018). On the other hand, P4 mirrored these alterations in the opposite direction of T, which could indicate an absence of ovulation. Furthermore, levels of E2 were significantly higher in WK PCOS (18%) and SHR PCOS (34%) groups, compared to respective controls. The higher elevation of E2 in SHR strain could be explained by the increase of aromatase activity compared to WK (Pietranera *et al.* 2011) and the consequent higher degree of T conversion into E2.

The effect of observed hormonal disturbances led to alteration of GC and TC layers thickness. Compared to respective controls, the GC layer thickness was lower in WK PCOS and SHR PCOS rats, while there was no difference between both control groups. However, compared to WK, the TC layer was thicker in WK PCOS, while SHR PCOS group did not show a statistically significant difference when compared to SHR group.

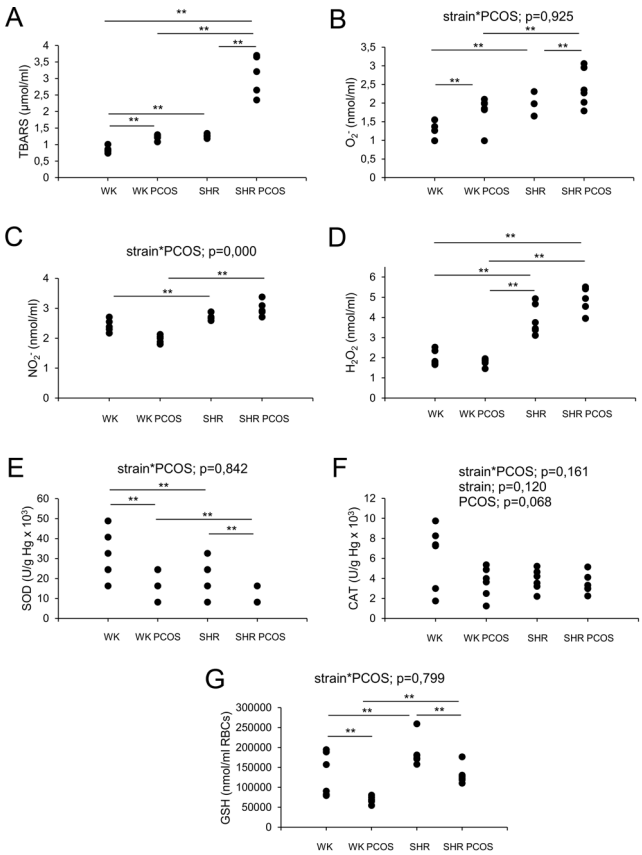

Figure 5 Oxidative stress parameters in blood of rats from WK, WK PCOS, SHR, and SHR PCOS groups. (A) Index of lipid peroxidation (expressed as TBARS); (B) levels of superoxide anion radical – O_2^-; (C) levels of nitrites – NO_2^-; (D) levels of hydrogen peroxide – H_2O_2; (E) activity of superoxide dismutase – SOD; (F) activity of catalase – CAT; (G) level of reduced glutathione – GSH. ** $P < 0.05$, two-way ANOVA was used for analysis; factor strain and factor PCOS were evaluated or Kruskal–Wallis test and *post hoc* Mann–Whitney analysis were performed.

TC layers were significantly thicker in SHR compared to WK. Thinning of GC layer and hyperthecosis, observed in WK PCOS, considered part of PCOS settings, was demonstrated in the hyperandrogenic PCOS women (Dadachanji *et al.* 2018) and confirmed by our ultrasonographical analysis. The thicker TC layer was suggested as an androgen source, attributed to increased steroidogenesis. However, in rat androgen PCOS models (Wu *et al.* 2019), the TC layer was also thicker, regardless of exogenous T administration. On the other hand, the thickened TC layer in SHR was firstlobserved in our study and could be to some extent related to increased androgen secretion in that strain. Although the GC were arranged in a significantly thinner layer, there was no further increase regarding TC layer thickness in SHR PCOS, which could be assumed to be an adaptation to hyperandrogenemia.

Observed alterations in follicle number implied that follicle recruitment in hyperandrogenemic PCOS state in both strains worsened the degree of atresia and lowered the number of healthy antral follicles, which could reach the preovulatory stadium. Furthermore, the presence of cysts and the absence of CL were also in accordance with lower P4 levels, which corresponds to PCOS (Bas *et al.* 2011). However, for the first time, this study revealed the difference between WK and SHR regarding the follicle number, and even though we evaluated only central sections, the difference was evident. To our knowledge, there are no literature data concerning strain differences in ovarian follicles count analysis in WK rats and SHR, so our results represent the first evidence on this topic.

The evaluation of ovarian central section diameters did not reveal a significant difference between WK and SHR, quite likely ultrasonographically measured ovarian D1. However, these two parameters showed a strong positive correlation ($R=0,7$; $P < 0.01$), which established rat ovary ultrasonography as quite a reliable method for ovarian diameters (and volume) analysis. The PCOS induction lowered significantly all investigated parameters except D2, while the strain differences between WK and SHR were observed only regarding OV/BW index. Besides the well-known parameter termed 'gonadosomatic index' (Alves *et al.* 2019), we tried to estimate a new parameter – OV/BW index, which gave a better insight into group differences. Therefore, we assumed that OV/BW index might be a useful tool for estimating OV alterations in PCOS rat studies.

Androgen levels could be associated with higher BP values: the blockade of androgen receptor decreased BP, while ovariectomized female SHR reached higher BP values after androgen administration (Reckelhoff *et al.* 1998). Moreover, male SHR had decreased BP after gonadectomy (Crofton *et al.* 1993), which undoubtedly links androgen levels and HT in both genders. In the last decades, a growing body of literature established the relationship between HT and hyperandrogenic status in reproductive-age females, summarized by Amiri and colleagues (Amiri *et al.* 2020). Although the mechanisms underlying that connection are not fully revealed, we tried to unriddle these complex networks, providing evidence from basic science, which could be at least the tiniest part of this puzzle. All examined parameters regarding BP were higher in SHR compared to WK. PCOS modeling increased systolic BP, HR, MAP, and PP in WK rats, as in our previous study (Joksimovic Jovic J, unpublished observations), while in SHR strain, MAP, HR, and PP were only increased. Observed data indicated that even before TE administration, SHR probably adapted to higher androgen levels, and further stimulation by TE had not influenced systolic (nor diastolic) BP in this strain. Furthermore, the fact that observed increase of BP parameters in WK PCOS achieved a similar level as SHR led us to assume that PCOS itself may aggravate BP levels toward those seen in an innately SHR. However, further studies

should investigate whether PCOS development and its manifestations in normotensive rats carry cardiovascular risk similar to that of SHR. A large Danish study, enrolling premenopausal women, reported elevated BP values and increased cardiovascular risk in PCOS patients (Glintborg *et al.* 2015). Moreover, even though some studies reported no difference in 24-h BP measurements between obese PCOS and non-PCOS women (Meyer *et al.* 2005), others demonstrated a modest elevation of systolic BP during the daytime, as well as MAP in young PCOS patients (Holte *et al.* 1996), independently from obesity. MAP levels in our study were affected by PCOS induction as well as by strain differences. Moreover, a significant interaction between the two investigated factors was registered, which puts the MAP in the focus of further investigations regarding PCOS.

Finally, the underlying mechanisms for these fluctuations could be found in OS parameter alterations. Regarding the most toxic and fast-acting radicals we measured, such as O_2^- and H_2O_2, SHR showed a marked increase of both. However, in both strains, PCOS induction induced the increase of O_2^-, but no H_2O_2 levels. OS directly influences the development of HT by free radicals damage of macromolecules and indirectly through redox-dependent vascular wall signaling (Münzel *et al.* 2017). The increase in lipid peroxidation was evident in both strains after PCOS induction and in SHR compared to WK in control conditions. However, levels of nitrites were surprisingly higher in the SHR strain. Studies regarding increased NO_2^- levels in SHR (Wu & Yen 1999) concluded that the observed increase of nitrites was probably compensatory to combat hypertensive state. A significant interaction between two analyzed factors, strain and PCOS in this study, was observed regarding the level of nitrites, which could put the role of vascular impairment underlying complex PCOS pathophysiology in focus. The observed decrease of SOD in SHR and SHR PCOS was in accordance with available literature (Wu *et al.* 2020). However, the CAT activity was not affected in SHR PCOS rats, which may be discussed as depletion of this antioxidative enzyme in the SHR strain. Furthermore, GSH was elevated in SHR compared to WK, although PCOS induction lowered GSH in both strains. The mentioned decrease was described by others in PCOS rodent models (Murri *et al.* 2013). The GSH increase in the SHR could be explained by the compensatory elevation of intracellular non-oxidative machinery via reduced glutathione cycle to combat pro-oxidative radicals and maintain reduced homeostasis in cells.

In conclusion, this investigation provided further insights into potential mechanisms involved in the hypertensive state observed in hyperandrogenic PCOS rats and into a closer relationship between these two pathologies in the sense of oxidative disturbance. This study may be an excellent base for further clinical investigations, regarding different PCOS phenotypes HT in order to evaluate the role of oxidative stress in cardiovascular risk management.

Data availability

The raw data for all results obtained in the study are provided in the Supplementary table.

Supplementary materials

This is linked to the online version of the paper at https://doi.org/10.1530/REP-21-0219.

Declaration of interest

The authors declare that there is no conflict of interest that could be perceived as prejudicing the impartiality of the research reported.

Funding

This work was supported by the Faculty of Medical Sciences (JP 01/20), the University of Kragujevac, Serbia and the Ministry of Education, Science, and Technological Development of the Republic of Serbia, contract number 451-03-9/2021-14/200007.

Author contribution statement

J J J designed a study, performed experiments, and wrote the manuscript; N J designed a study and performed experiments; J S designed a study and performed experiments; V Z designed a study and performed experiments; M N designed a study and performed experiment; J R designed a study and performed experiments; N R designed a study and performed experiments; K A collected literature data and supervised text; T D T collected literature data and supervised text; and V M and V J designed and supervised the study; and B M performed statistical analysis and supervised the text. All authors have read and approved the final version of the manuscript and agreed with the order of presentation of the authors.

Acknowledgement

The authors would like to thank Dusan Tomasevic for technical support.

References

Aguilar E, Rodriguez Padilla ML, Bellido C, Tena-Sempere M & Pinilla L 1992 Changes in follicle-stimulating hormone secretion in spontaneously hypertensive rats. *Neuroendocrinology* **56** 85–93. (https://doi.org/10.1159/000126212)

Aladashvili-Chikvaidze N, Kristesashvili J & Gegechkori M 2015 Types of reproductive disorders in underweight and overweight young females and correlations of respective hormonal changes with BMI. *Iranian Journal of Reproductive Medicine* **13** 135–140.

Alves ED, Bonfá ALO, Pigatto GR, Anselmo-Franci JA, Achcar JA, Parizotto NA & Montrezor LH 2019 Photobiomodulation can improve

ovarian activity in polycystic ovary syndrome-induced rats. *Journal of Photochemistry and Photobiology: B, Biology* **194** 6–13. (https://doi.org/10.1016/j.jphotobiol.2019.03.006)

Amiri M, Ramezani Tehrani F, Behboudi-Gandevani S, Bidhendi-Yarandi R & Carmina E 2020 Risk of hypertension in women with polycystic ovary syndrome: a systematic review, meta-analysis and meta-regression. *Reproductive Biology and Endocrinology* **18** 23. (https://doi.org/10.1186/s12958-020-00576-1)

Auclair C & Voisin E 1985 Nitroblue tetrazolium reduction. In *Handbook of Methods for Oxygen Radical Research*, pp. 123–132. Ed **A Greenwald.** Boca Raton: CRC Press Press.

Bas D, Abramovich D, Hernandez F & Tesone M 2011 Altered expression of Bcl-2 and Bax in follicles within dehydroepiandrosterone-induced polycystic ovaries in rats. *Cell Biology International* **35** 423–429. (https://doi.org/10.1042/CBI20100542)

Beutler E 1982 Catalase. In *Red Cell Metabolism, A Manual of Biochemical Methods*, 3rd ed., pp. 105–106. New York: Grune and Stratton.

Beutler E 1984 Superoxide dismutase. In *Red Cell Metabolism, A Manual of Biochemical Methods*, 2nd ed., pp. 83–85. Ed **E Beutler.** New York: Grune & Stratton.

Chen MJ, Yang WS, Yang JH, Chen CL, Ho HN & Yang YS 2007 Relationship between androgen levels and blood pressure in young women with polycystic ovary syndrome. *Hypertension* **49** 1442–1447. (https://doi.org/10.1161/HYPERTENSIONAHA.106.083972)

Chen X, Huang L, Tan HY, Li H, Wan Y, Cowley M, Veldhuis JD & Chen C 2017 Deficient melanocortin-4 receptor causes abnormal reproductive neuroendocrine profile in female mice. *Reproduction* **153** 267–276. (https://doi.org/10.1530/REP-16-0341)

Crofton JT, Ota M & Share L 1993 Role of vasopressin, the renin-angiotensin system and sex in Dahl salt-sensitive hypertension. *Journal of Hypertension* **11** 1031–1038. (https://doi.org/10.1097/00004872-199310000-00005)

Dadachanji R, Shaikh N & Mukherjee S 2018 Genetic variants associated with yperandrogenemia in PCOS pathophysiology. *Genetics Research International* **2018** 7624932. (https://doi.org/10.1155/2018/7624932)

Dickhout JG & Lee RM 1998 Blood pressure and heart rate development in young spontaneously hypertensive rats. *American Journal of Physiology* **274** H794–H800. (https://doi.org/10.1152/ajpheart.1998.274.3.H794)

Elting MW, Korsen TJ, Bezemer PD & Schoemaker J 2001 Prevalence of diabetes mellitus, hypertension and cardiac complaints in a follow-up study of a Dutch PCOS population. *Human Reproduction* **16** 556–560. (https://doi.org/10.1093/humrep/16.3.556)

Feng M, Whitesall S, Zhang Y, Beibel M, D'Alecy L & DiPetrillo K 2008 Validation of volume-pressure recording tail-cuff blood pressure measurements. *American Journal of Hypertension* **21** 1288–1291. (https://doi.org/10.1038/ajh.2008.301)

Furedi N, Miko A, Aubrecht B, Gaszner B, Feller D, Rostas I, Tenk J, Soos S, Balasko M, Balogh A *et al.* 2016 Regulatory alterations of energy homeostasis in spontaneously hypertensive rats (SHR). *Journal of Molecular Neuroscience* **59** 521–530. (https://doi.org/10.1007/s12031-016-0771-2)

Ghowsi M, Khazali H & Sisakhtnezhad S 2018 Evaluation of TNF-α and IL-6 mRNAs expressions in visceral and subcutaneous adipose tissues of polycystic ovarian rats and effects of resveratrol. *Iranian Journal of Basic Medical Sciences* **21** 165–174. (https://doi.org/10.22038/IJBMS.2017.24801.6167)

Glintborg D, Hass Rubin K, Nybo M, Abrahamsen B & Andersen M 2015 Morbidity and medicine prescriptions in a nationwide Danish population of patients diagnosed with polycystic ovary syndrome. *European Journal of Endocrinology* **172** 627–638. (https://doi.org/10.1530/EJE-14-1108)

Green LC, Wagner DA, Glogowski J, Skipper PL, Wishnok JS &Tannenbaum SR 1982 Analysis of nitrate, nitrite, and [15N]nitrate in biological fluids. *Analytical Biochemistry* **126** 131–138. (https://doi.org/10.1016/0003-2697(82)90118-X)

Holte J, Gennarelli G, Berne C, Bergh T & Lithell H 1996 Elevated ambulatory day-time blood pressure in women with polycystic ovary syndrome: a sign of a pre-hypertensive state? *Human Reproduction* **11** 23–28. (https://doi.org/10.1093/oxfordjournals.humrep.a019028)

IJzerman RG, Stehouwer CD, de Geus EJ, van Weissenbruch MM, Delemarre-van de Waal HA & Boomsma DI 2003 Low birth weight is associated with increased sympathetic activity: dependence on genetic factors. *Circulation* **108** 566–571. (https://doi.org/10.1161/01.CIR.0000081778.35370.1B)

Iwasa T, Matsuzaki T, Yano K, Yanagihara R, Tungalagsuvd A, Munkhzaya M, Mayila Y, Kuwahara A & Irahara M 2017 The effects of chronic testosterone administration on body weight, food intake, and adipose tissue are changed by estrogen treatment in female rats. *Hormones and Behavior* **93** 53–61. (https://doi.org/10.1016/j.yhbeh.2017.05.008)

Johansson J, Feng Y, Shao R, Lönn M, Billig H & Stener-Victorin E 2010 Intense electroacupuncture normalizes insulin sensitivity, increases muscle GLUT4 content, and improves lipid profile in a rat model of polycystic ovary syndrome. *American Journal of Physiology: Endocrinology and Metabolism* **299** E551–E559. (https://doi.org/10.1152/ajpendo.00323.2010)

Joksimovic J, Selakovic D, Jovicic N, Mitrovic S, Mihailovic V, Katanic J, Milovanovic D & Rosic G 2019 Exercise attenuates anabolic steroids-induced anxiety via hippocampal NPY and MC4 receptor in rats. *Frontiers in Neuroscience* **13** 172. (https://doi.org/10.3389/fnins.2019.00172)

Joksimovic Jovic J, Sretenovic J, Jovic N, Rudic J, Zivkovic V, Srejovic I, Mihajlovic K, Draginic N, Andjic M, Milinkovic M *et al.* 2021 Cardiovascular properties of the androgen-induced PCOS model in rats: the role of oxidative stress. *Oxidative Medicine and Cellular Longevity* **2021** 8862878. (https://doi.org/10.1155/2021/8862878)

Kalhori Z, Azadbakht M, Soleimani Mehranjani M & Shariatzadeh MA 2018 Improvement of the folliculogenesis by transplantation of bone marrow mesenchymal stromal cells in mice with induced polycystic ovary syndrome. *Cytotherapy* **20** 1445–1458. (https://doi.org/10.1016/j.jcyt.2018.09.005)

Lansdown A & Rees DA 2012 The sympathetic nervous system in polycystic ovary syndrome: a novel therapeutic target? *Clinical Endocrinology* **77** 791–801. (https://doi.org/10.1111/cen.12003)

Liu G, Shi F, Blas-Machado U, Duong Q, Davis VL, Foster WG & Hughes CL 2005 Ovarian effects of a high lactose diet in the female rat. *Reproduction, Nutrition, Development* **45** 185–192. (https://doi.org/10.1051/rnd:2005010)

Marchesan LB & Spritzer PM 2019 ACC/AHA 2017 definition of high blood pressure: implications for women with polycystic ovary syndrome. *Fertility and Sterility* **111** 579.e1–587.e1. (https://doi.org/10.1016/j.fertnstert.2018.11.034)

Marcondes FK, Bianchi FJ & Tanno AP 2002 Determination of the estrous cycle phases of rats: some helpful considerations. *Brazilian Journal of Biology* **62** 609–614. (https://doi.org/10.1590/s1519-69842002000400008)

Martínez LA, Cifuentes F & Morales MA 2019 Ganglionic long-term potentiation in prehypertensive and hypertensive stages of spontaneously hypertensive rats depends on GABA modulation. *Neural Plasticity* **2019** 7437894. (https://doi.org/10.1155/2019/7437894)

McCord JM & Fridovich I 1969 The utility of superoxide dismutase in studying free radical reactions I radicals generated by the interaction of sulfite, dimethyl sulfoxide, and oxygen. *Journal of Biological Chemistry* **244** 6056–6063. (https://doi.org/10.1016/S0021-9258(18)63505-7)

Meyer C, McGrath BP & Teede HJ 2005 Overweight women with polycystic ovary syndrome have evidence of subclinical cardiovascular disease. *Journal of Clinical Endocrinology and Metabolism* **90** 5711–5716. (https://doi.org/10.1210/jc.2005-0011)

Misra HP & Fridovich I 1972 The role of superoxide-anion in the autoxidation of epinephrine and a simple assay for superoxide dismutase. *Journal of Biological Chemistry* **247** 3170–3175. (https://doi.org/10.1016/S0021-9258(19)45228-9)

Mumm H, Kamper-Jørgensen M, Nybo Andersen AM, Glintborg D & Andersen M 2013 Birth weight and polycystic ovary syndrome in adult life: a register-based study on 523,757 Danish women born 1973–1991. *Fertility and Sterility* **99** 777–782. (https://doi.org/10.1016/j.fertnstert.2012.11.004)

Münzel T, Camici GG, Maack C, Bonetti NR, Fuster V & Kovacic JC 2017 Impact of oxidative stress on the heart and vasculature: part 2 of a 3-part series. *Journal of the American College of Cardiology* **70** 212–229. (https://doi.org/10.1016/j.jacc.2017.05.035)

Murri M, Luque-Ramírez M, Insenser M, Ojeda-Ojeda M& Escobar-Morreale HF 2013 Circulating markers of oxidative stress and polycystic ovary syndrome (PCOS): a systematic review and meta-analysis. *Human Reproduction Update* **19** 268–288. (https://doi.org/10.1093/humupd/dms059)

Nardo LG, Buckett WM & Khullar V 2003 Determination of the best-fitting ultrasound formulaic method for ovarian volume measurement in women with polycystic ovary syndrome. *Fertility and Sterility* **79** 632–633. (https://doi.org/10.1016/s0015-0282(02)04801-x)

Ohkawa H, Ohishi N & Yagi K 1979 Assay for lipid peroxides in animal tissues by thiobarbituric acid reaction. *Analytical Biochemistry* **95** 351–358. (https://doi.org/10.1016/0003-2697(79)90738-3)

Orio F, Palomba S & Colao A 2006 Cardiovascular risk in women with polycystic ovary syndrome. *Fertility and Sterility* **86** (Supplement 1) S20–S21. (https://doi.org/10.1016/j.fertnstert.2006.03.003)

Pasquali R 2006 Obesity and androgens: facts and perspectives. *Fertility and Sterility* **85** 1319–1340. (https://doi.org/10.1016/j.fertnstert.2005.10.054)

Pick E & Keisari Y 1980 A simple colorimetric method for the measurement of hydrogen peroxide produced by cells in culture. *Journal of Immunological Methods* **38** 161–170. (https://doi.org/10.1016/0022-1759(80)90340-3)

Pietranera L, Bellini MJ, Arévalo MA, Goya R, Brocca ME, Garcia-Segura LM & De Nicola AF 2011 Increased aromatase expression in the hippocampus of spontaneously hypertensive rats: effects of estradiol administration. *Neuroscience* **174** 151–159. (https://doi.org/10.1016/j.neuroscience.2010.11.044)

Pinilla L, Rodriguez-Padilla ML, Sanchez-Criado J, Gaytan F & Aguilar E 1992 Mechanism of reproductive deficiency in spontaneously hypertensive rats. *Physiology and Behavior* **51** 99–104. (https://doi.org/10.1016/0031-9384(92)90209-k)

Pinilla L, Castellano JM, Romero M, Tena-Sempere M, Gaytán F & Aguilar E 2009 Delayed puberty in spontaneously hypertensive rats involves a primary ovarian failure independent of the hypothalamic KiSS-1/GPR54/GnRH system. *Endocrinology* **150** 2889–2897. (https://doi.org/10.1210/en.2008-1381)

Qiu S, Wu C, Lin F, Chen L, Huang Z & Jiang Z 2009 Exercise training improved insulin sensitivity and ovarian morphology in rats with polycystic ovary syndrome. *Hormone and Metabolic Research* **41** 880–885. (https://doi.org/10.1055/s-0029-1234119)

Reckelhoff JF, Zhang H & Granger JP 1998 Testosterone exacerbates hypertension and reduces pressure-natriuresis in male spontaneously hypertensive rats. *Hypertension* **31** 435–439. (https://doi.org/10.1161/01.hyp.31.1.435)

Roa J & Herbison AE 2012 Direct regulation of GnRH neuron excitability by arcuate nucleus POMC and NPY neuron neuropeptides in female mice. *Endocrinology* **153** 5587–5599. (https://doi.org/10.1210/en.2012-1470)

Rodgers RJ, Suturina L, Lizneva D, Davies MJ, Hummitzsch K, Irving-Rodgers HF & Robertson SA 2019 Is polycystic ovary syndrome a 20th century phenomenon? *Medical Hypotheses* **124** 31–34. (https://doi.org/10.1016/j.mehy.2019.01.019)

Simão VA, de Almeida Chuffa LG & Cherici Camargo IC 2016 Ovarian sex steroid receptors and sex hormones in androgenized rats. *Reproduction* **152** 545–559. (https://doi.org/10.1530/REP-16-0233)

Stener-Victorin E, Padmanabhan V, Walters KA, Campbell RE, Benrick A, Giacobini P, Dumesic DA & Abbott DH 2020 Animal models to understand the etiology and pathophysiology of polycystic ovary syndrome. *Endocrine Reviews* **41** 41538–41576. (https://doi.org/10.1210/endrev/bnaa010)

Walters KA, Allan CM & Handelsman DJ 2012 Rodent models for human polycystic ovary syndrome. *Biology of Reproduction* **86** 149, 1–12. (https://doi.org/10.1095/biolreprod.111.097808)

Wang ET, Ku IA, Shah SJ, Daviglus ML, Schreiner PJ, Konety SH, Dale Williams OD, Siscovick D & Bibbins-Domingo K 2012 Polycystic ovary syndrome is associated with higher left ventricular mass index: the CARDIA women's study. *Journal of Clinical Endocrinology and Metabolism* **97** 4656–4662. (https://doi.org/10.1210/jc.2012-1597)

Wu CC & Yen MH 1999 Higher level of plasma nitric oxide in spontaneously hypertensive rats. *American Journal of Hypertension* **12** 476–482. (https://doi.org/10.1016/s0895-7061(99)00008-4)

Wu C, Jiang F, Wei K, Lin F& Jiang Z 2019 Effects of exercise combined with finasteride on hormone and ovarian function in polycystic ovary syndrome rats. *International Journal of Endocrinology* **2019** 8405796. (https://doi.org/10.1155/2019/8405796)

Wu G, Hu X, Ding J & Yang J 2020 The effect of glutamine on dehydroepiandrosterone-induced polycystic ovary syndrome rats. *Journal of Ovarian Research* **13** 57. (https://doi.org/10.1186/s13048-020-00650-7)

Zhu S, Zhang B, Jiang X, Li Z, Zhao S, Cui L & Chen ZJ 2019 Metabolic disturbances in non-obese women with polycystic ovary syndrome: a systematic review and meta-analysis. *Fertility and Sterility* **111** 168–177. (https://doi.org/10.1016/j.fertnstert.2018.09.013)

Zuo T, Zhu M & Xu W 2016 Roles of oxidative stress in polycystic ovary syndrome and cancers. *Oxidative Medicine and Cellular Longevity* **2016** 8589318. (https://doi.org/10.1155/2016/8589318)

Received 24 May 2021
First decision 8 June 2021
Revised manuscript received 6 November 2021
Accepted 11 November 2021